Time-Resolving Analysis of Cryotropic Gelation of Water/Poly(vinyl alcohol) Solutions via Small-Angle Neutron Scattering

Finizia Auriemma,*,† Claudio De Rosa,† Rosa Ricciardi,† Fabrizio Lo Celso,‡ Roberto Triolo,‡ and Vitaly Pipich§

Dipartimento di Chimica Paolo Corradini, Università di Napoli Federico II, Complesso Monte Sant' Angelo, via Cintia, 80126 Napoli, Italy, Dipartimento di Chimica Fisica Filippo Accascina, Università degli Studi di Palermo, Viale delle Scienze, Ed. 17, 90128 Palermo, Italy, and Institut für Festkörperforschung, Forschungszentrum Jülich GmbH, D-52425 Jülich, Germany

Received: August 9, 2007; In Final Form: October 20, 2007

The structural transformations occurring in initially homogeneous aqueous solutions of poly(vinyl alcohol) (PVA) through application of freezing (−13 °C) and thawing (20 °C) cycles is investigated by time resolving small-angle neutron scattering (SANS). These measurements indicate that formation of gels of complex hierarchical structure arises from occurrence of different elementary processes, involving different length and time scales. The fastest process that could be detected by our measurements during the first cryotropic treatment consists of the crystallization of the solvent. However, solvent crystallization is incomplete, and an unfrozen liquid microphase more concentrated in PVA than the initial solution is also formed. Crystallization of PVA takes place inside the unfrozen liquid microphase and is slowed down because of formation of a microgel fraction. Water crystallization takes place in the early 10 min of the treatment of the solution at subzero temperatures, and although below 0 °C the PVA solutions used for preparation of cryogels should be below the spinodal curve, occurrence of liquid−liquid phase separation could not be detected in our experiments. Upon thawing, ice crystals melt, and transparent gels are obtained that become opaque in ∼200 min, due to a slow and progressive increase of the size of microheterogeneities (dilute and dense regions) imprinted during the fast freezing by the crystallization of water. During the permanence of these gels at room temperature (for hours), the presence of a high content of water (higher than 85% by mass) prevents further crystallization of PVA. Crystallization of PVA, in turn, is resumed by freezing the gels at subzero temperatures, after water crystallization and consequent formation of an unfrozen microphase. The kinetic parameters of PVA crystallization during the permanence of these gels at subzero temperatures are the same shown by PVA during the first freezing step of the solutions.

Introduction

The formation of physical gels from water solutions of poly(vinyl alcohol) (PVA) has been largely studied. In fact, it is well-known that aqueous PVA solutions undergo gelation upon cooling. In these gels the tie points are generally fringed micelle-like PVA crystallites. In particular, Komatsu et al.[1] found that the phase diagram of this system shows an upper critical solution temperature, in which the spinodal curve crosses the sol−gel transition curve. This phase diagram is redrawn in Figure 1.

It is apparent that gelation takes place both below and above the spinodal curve, indicating that gels may be formed either accompanied by spinodal decomposition or without liquid−liquid phase separation, respectively.[1] In both cases, crystallites act as tie points of the network, and these crystals correspond to the monoclinic form of atactic PVA with chains in trans-planar conformation,[1,2] as studied by Bunn.[3] It has been shown that the existence of a region in the phase diagram in which gelation is accompanied by spinodal decomposition[4] does not mean that the development of an interconnected structure in the polymer-rich phase is the origin of gelation. However, the supramolecular structure of the hydrogels that develops in this region is considerably different and more heterogeneous than the structure of the statistical gel that develops in the region of the phase diagram above the spinodal curve, without liquid−liquid phase separation.[1]

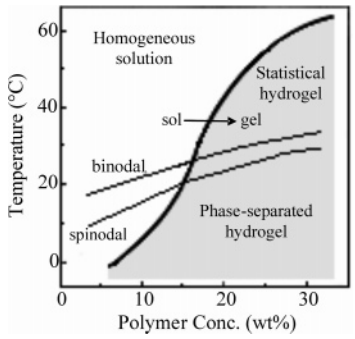

Figure 1. Sol−gel transition curve, spinodal, and binodal of the water/PVA binary system (redrawn from ref 1).

In water/PVA systems, gelation may also be induced by cryogenic treatments, i.e., at temperatures where the formation of ice crystals takes place.[5−8] The cryogenic treatment basically consists of freezing an initially homogeneous polymer solution

* To whom correspondence should be addressed. Telephone: ++39 081 674341. Fax ++39 081 674090. E-mail: finizia.auriemma@unina.it.
† Università di Napoli Federico II.
‡ Università degli Studi di Palermo.
§ Forschungszentrum Jülich GmbH.

10.1021/jp0763984 CCC: $40.75
Published on Web 12/29/2007

at low temperatures, storing it in the frozen state for a definite time, and finally defrosting it. Freezing is generally performed at high cooling rates, and although strong physical gels are obtained already by imposing a single freeze/thaw cycle, in order to improve the strength of these gels, freezing and thawing are repeated a number of times.[5,6]

The freeze/thaw treatment is able to produce heterogeneous materials, with a high water content (85−90% by weight) that exhibit a different morphology compared to the more conventional gels obtained from nonfrozen systems.[5,6,9] The main characteristic feature of PVA cryogels is a network including interconnected micro- and macropores.[6] In PVA hydrogels obtained by cryotropic treatments, this structure induces outstanding properties such as high modulus, rubber elasticity, and mechanical stability over a large range of deformation and temperatures. These properties, along with a lack of toxicity, biocompatibility, and large water content, make freeze/thaw PVA hydrogels attractive matrices for chromatography, hosts for biological nanoparticles, and cell scaffolds in tissue engineering.[5−7]

The outstanding properties of these systems depend on their complex architecture, where PVA chains and water molecules are organized over different hierarchical length scales. The heterogeneous structure of freeze/thaw PVA hydrogels is very similar to the structure of PVA gels formed in (60/40 v/v) mixtures of dimethyl sulfoxide (DMSO) and water studied by Kanaya et al. using wide-[10,11] and small-angle[10−12,13] neutron scattering and light-scattering[11,12,14] techniques. In fact, both kinds of PVA gels consist of two bicontinuous phases, namely, polymer-rich and polymer-poor regions.[6,9,15] The polymer-rich regions (of average dimensions on the order of microns)[16] include crystallites of PVA 3−4 nm[17,18] in size and a swollen amorphous phase, the average distance between crystallites being on the order of 10−20 nm.[15] The polymer-poor regions, in turn, allow almost unhindered diffusion of large and small molecules.[5,6,19,20] The tie-points of the macroscopic network are essentially PVA crystallites connected by portions of chains swollen by the solvent.[9,17,18] The size and amount of PVA crystalline aggregates in freeze/thaw PVA hydrogels play an important role in their performances in application, since the dimensional stability, toughness, strength to external stresses, and thermal stability of PVA cryogels are critically dependent on these parameters.[2,19]

The origin and the mechanism of formation of such an open porous structure are still unclear. The formation of the heterogeneous structure of PVA hydrogels, indeed, is the result of the occurrence of at least three concomitant and at the same time conflicting processes, namely, crystallization of the solvent, liquid−liquid phase separation, and crystallization of PVA. At subzero temperatures, indeed, the solutions having the typical concentrations used for preparation of PVA cryogels are below the spinodal curve.[1] Therefore, during the freezing and the successive permanence of the solution at subzero temperatures, beside the crystallization of the solvent and of PVA, a liquid−liquid phase separation may also occur (see Figure 1).

Using time-resolving (TR) small-angle neutron scattering (SANS), in a recent investigation we have shown that PVA crystallization plays an important role in the formation of these gels.[21] In particular, we have shown that PVA crystallites are formed already during the prolonged storage of the homogeneous solutions at subzero temperatures and that these crystallites are responsible for the development of a stable gel network upon thawing, provided that the concentration of the solution is higher than a critical value. At these temperatures, most of the solvent, water, is frozen, while the solute is concentrated in small regions constituting the so-called "nonfrozen liquid microphase" of eutectic composition.[6] Crystallization of PVA takes place inside these regions. However, although the temperature of the system is likely below the eutectic temperature, the crystallization of PVA may not be complete, because the unfrozen liquid microphase jellifies, preventing the attainment of thermodynamic equilibrium. Therefore, formation of the gels upon defrosting is the result of two incomplete processes, namely, incomplete water crystallization and incomplete PVA crystallization.

Our early investigation[21] was mainly focused on the study of the kinetics of formation of PVA aggregates responsible for the development of a stable gel network in the unfrozen liquid microphase during the permanence of PVA solutions at subzero temperatures, by performing SANS measurements restricted to the length scale below 100 nm, which is useful for analysis of the development of PVA crystallites. In this paper, we have extend the TR-SANS analysis of the cryotropic gelation mechanism of PVA/water solutions to a wider range of length scales and have followed the structural transformations occurring in this system not only during the permanence of the solutions at subzero temperature but also during the successive thawing and permanence of the PVA/water binary system at room temperature. Furthermore, the gels obtained upon imposing a single freeze/thaw treatment have been analyzed using TR-SANS also during a successive freezing treatment. Understanding the factors that govern the cryogelation mechanism of PVA homogeneous solutions is useful both in fundamental studies of the phenomena subtending the formation of macroporous gels in polymeric materials and from an applicative standpoint, because it may allow for the control of the final architecture of cryogels by simply tuning the conditions of preparation, with the aim to obtain materials with enhanced properties for tailored applications.

Experimental Section

Atactic PVA used for the analysis was purchased from Aldrich. The average molecular weight, M_w, was 104 000 and the degree of hydrolysis was 98−99%. The ^{13}C NMR spectrum analysis of PVA in deuterated water solution shows that the percentages of *mm*, *mr*, and *rr* configurational triads were 22.1, 50.1, and 27.8%, respectively, confirming that the polymer was atactic.

Aqueous solutions at three different concentrations of PVA of 5.03, 10.11, and 14.22% (w/w) were prepared by dissolving the PVA polymer in heavy water (Aldrich, stated purity 99.8%, molar mass 20.03 g mol^{-1}) at 96 °C, under reflux and stirring, for about 3 h. The volume fractions of PVA in the solutions, Φ_{PVA},corresponded to 0.042, 0.086, and 0.12, respectively, assuming values of density of crystalline PVA[3] and heavy water equal to 1.348 and 1.12 g/cm^3, respectively. In all cases, a homogeneous solution was obtained that did not jellify even after 1 month at room temperature in sealed vials in order to prevent water evaporation. Moreover, whereas the solutions with $\Phi_{PVA} = 0.086$ and 0.12 formed gels by cryotropic treatments, the solution with $\Phi_{PVA} = 0.042$ was unable to jellify under the same processing conditions.[21]

Small-angle neutron scattering measurements were performed at the KWS1 facility located at the Forschungszentrum of Jülich, Germany. Solutions were placed in 2 mm path length Hellma quartz cells. Neutrons with an average wavelength λ of 7 Å and a wavelength spread $\Delta\lambda/\lambda \leq 0.2$ were used. Measurements wereperformed using a two-dimensional array detector at three

different sample-to-detector distances of 2, 4, and 20 m. These configurations allowed collecting of the scattered neutrons in the range of scattering vector q between 0.02 and 1.2 nm^{-1} ($q = 4\pi \sin\theta/\lambda$ where 2θ is the scattering angle). The gelation kinetics were followed by TR-SANS measurements. More precisely, during freezing, data collection was started immediately after quenching the water/PVA system from room temperature to a precooled thermostatic bath at −13 °C, whereas during thawing the measures were started immediately after quenching the frozen system from −13 °C to a preheated thermostatic bath at 20 °C. The temperature control of the thermostatic bath was ±1°C. The time of each measurement was set equal to 36, 36, and 60 s, depending on the sample to detector distance of 2, 4, and 20 m, respectively. The gelation kinetics was followed for at least 1 h during freezing and thawing. Reproducibility of data was checked by repeating the experiments on at least two different solutions with the same PVA concentration.

Raw data were corrected for electronic background and empty cell scattering. Detector sensitivity corrections and transformation to absolute scattering cross sections $(d\sigma/d\Omega)(q)$ were made with a secondary Lupolene standard. Data were then radially averaged and absolute scattering cross sections were obtained.

Results and Discussion

Shape Analysis of SANS Curves. The SANS scattering cross sections of the initially homogeneous solution with $\Phi_{PVA} = 0.086$ ($t = 0$) and of the same solution after 10, 14, and 30 min of permanence at −13 °C are compared in Figure 2A. It is apparent that the SANS curve of the initial solution shows an upturn at q less than 0.04 nm^{-1}, presumably because the PVA chains do not exist in solution as isolated random coils but form superstructures (curve a of Figure 2A).[22] The scattering cross section of the solution increases with increasing the time of permanence at −13 °C rather sharply in the early 10−20 min (curves b, c of Figure 2A) achieving constant values after 30 min (curve d of Figure 2A). After 30 min, indeed, the SANS curve becomes practically coincident with that of the solution kept at −13 °C for 390 min (compare curves a and d of Figure 3A).

These data essentially confirm the results obtained in ref 21. Namely, the increase of scattering cross section during freezing is essentially due to structural changes that occur in the solution associated with the crystallization of the water. This is also confirmed in Figure 3A, which shows that the SANS curve of the frozen solution kept at −13 °C for 390 min (curve a of Figure 3A) is quite different from that of the frozen solvent (curve b of Figure 3A). In fact, whereas the scattering cross section of ice for $q < 0.1$ nm^{-1} is characterized by a q^{-4} dependence typical of crystals, the scattering cross section of the frozen solution exhibits two distinct regimes as a function of q, separated by a knee located at $q_{knee} \approx 0.07$ nm^{-1}. In the q range between 0.35 and 0.07 nm^{-1}, the scattered intensity decays as approximately $q^{-3.7}$, whereas at low q values ($0.02 < q < 0.07$ nm^{-1}) the intensity decays approximately as $q^{-2.2}$. This indicates that the frozen solution is nonuniform, being characterized by the presence of large heterogeneities within the ice matrix constituted by the unfrozen liquid microphase, of characteristic size L approximately equal to $(2\pi/q_{knee} \approx)$ 75−80 nm.[21]

A more quantitative parameter may be found through the fit of the experimental SANS data (points a in Figure 3A) to a hierarchical structural model[23] that takes into account the existence of a network of fractal aggregates of size ξ greater than $2\pi/q_{min}$ (≈300 nm, with q_{min} the lowest value of q experimentally achieved) formed by monodisperse primary objects of spherical shape of radius r ($=L/2$)[23] (the fitting curve is indicated by the solid line b of Figure 3A).[21] According to this model, the dimensionality of interfacial region D_s of the primary objects of radius r constituting the unfrozen liquid microphase with the ice matrix determines the power law dependence of the scattering cross section at large scattering vector, whereas the power law exponent of the scattering cross section at $q < 0.07$ nm^{-1} is determined by the value of D, an exponent describing how the cluster mass scales with the cluster size ($M \propto \xi^D$) (i.e., $d\sigma/d\Omega$ for $\xi^{-1} < q < r^{-1}$ scales as q^{-D}).[23] The fitting of experimental data from the $\Phi_{PVA} = 0.086$ frozen system to the above-described hierarchical structural model gives $D_s = 3.67 \pm 0.04$, $r = 45.6 \pm 0.1$ nm and $D = 2.19 \pm 0.01$.[21]

The formation of clusters of dimensions larger than 300 nm in the matrix of ice crystals built up of primary regions of size of 80−90 nm constituting the unfrozen liquid microphase is confirmed by the experimental observation, shown in Figure 3B, that the SANS curve of the frozen solution with $\Phi_{PVA} = 0.086$ (curve b) is similar to that of the frozen solution with $\Phi_{PVA} = 0.12$ (curve c), and quite different from the SANS pattern of the frozen solution with $\Phi_{PVA} = 0.042$ (curve a). In fact, whereas the two more concentrated solutions form a gel upon defrosting, the solution with $\Phi_{PVA} = 0.042$ is unable to form a macroscopic gel under the same cryotropic treatment. In the latter case (curve a of Figure 3B), the SANS scattering

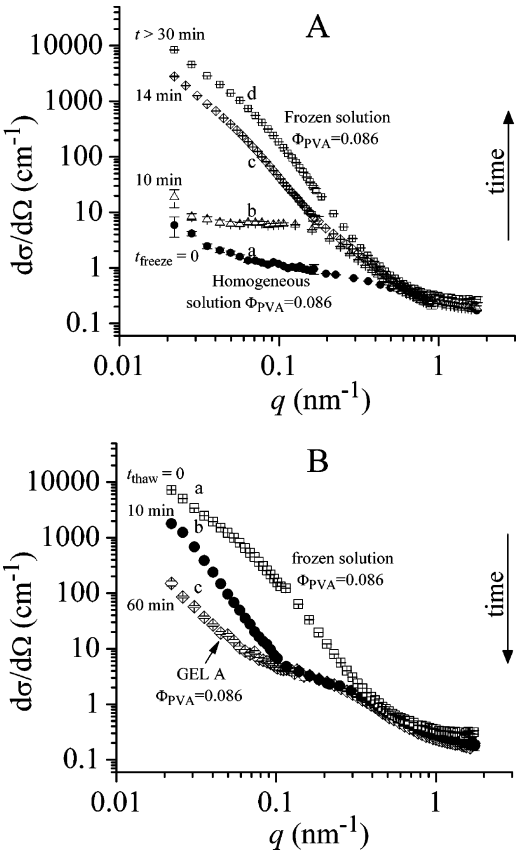

Figure 2. Change of the scattering cross section as a function of the scattering vector q (A) from the initial solution with $\Phi_{PVA} = 0.086$ at room temperature ($t_{freeze} = 0$) (a) and during the permanence of the solution at −13 °C, after 10 min (b), 14 min (c), and 30 min (d) and (B) from the frozen solution after 390 min at −13 °C ($t_{thaw} = 0$) (a) and during the permanence at 20 °C after 10 min (b) and 60 min (c). The transparent gel obtained after 60 min at 20 °C is indicated as GEL A. The elapsed time (min) after the quenching at −13 °C (A) and 20 °C (B) is also indicated.

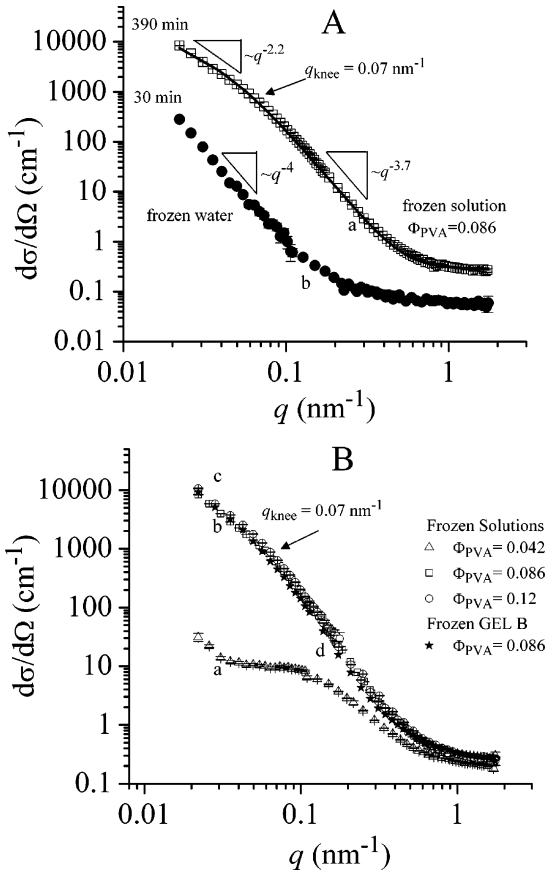

Figure 3. Comparison of the scattering cross section (A) of the frozen solution with $\Phi_{PVA} = 0.086$ after 390 min at −13 °C (curve a) with the SANS pattern of frozen D_2O after 30 min at −13 °C (curve b) and (B) of the frozen solution with $\Phi_{PVA} = 0.086$ after 390 min at −13 °C (curve b, □) with those of frozen solutions with $\Phi_{PVA} = 0.042$ (curve a, △) and $\Phi_{PVA} = 0.12$ (curve c, ○) after ≈ 90 and ≈120 min at −13 °C, respectively, and of the frozen GEL B with $\Phi_{PVA} = 0.086$ (curve d, ★) after 45 min at −13 °C. The elapsed time (min) after the quenching at −13 °C of pure D_2O and of PVA solutions is indicated. In part A, the inflection point q_{knee} at 0.07 nm^{-1} and the power law dependence in q of the scattering cross section from the $\Phi_{PVA} = 0.086$ frozen solution in the two regions separated by the inflection point (curve a) and from the frozen water for $q < 0.1$ nm^{-1} (curve b) are also indicated. The solid line (curve a of part A) is the fit of experimental data from the $\Phi_{PVA} = 0.086$ solution in the frozen state to a hierarchical structural model[23] given in ref 21.

pattern is similar to that of the $\Phi_{PVA} = 0.086$ PVA system after 10 min at −13 °C (curve b of Figure 2A), corresponding to the $\Phi_{PVA} = 0.086$ system not yet completely structured. This indicates that, in the frozen system with $\Phi_{PVA} = 0.042$, the unfrozen liquid microphase forms small clusters inside the ice matrix. In other terms, for polymer concentrations below a critical value, the total volume of the unfrozen liquid microphase is below a percolation threshold. In fact, during the freezing of the solution, water crystallization induces a progressive increase of the PVA concentration in the surrounding solution, reaching the eutectic composition. When the concentration of PVA in the system is below a threshold limit, we expect that also the volume fraction of the unfrozen liquid microphase is low and therefore unable to form at least one infinite cluster in the system (i.e., to form a gel). Probably clusters are still formed, but they have finite dimensions.

In Figure 2B, the SANS pattern of the PVA system with $\Phi_{PVA} = 0.086$ frozen for 390 min at −13 °C measured at the beginning of the thawing step ($t_{thaw} = 0$) (curve a) is compared with the SANS curves recorded during the storage of the system

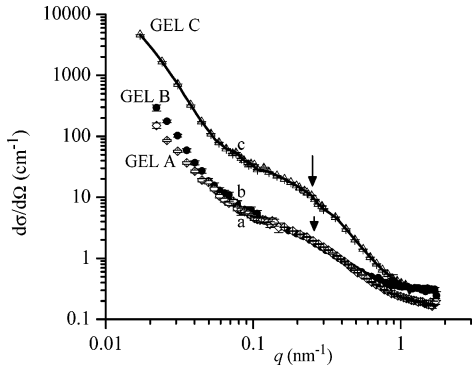

Figure 4. Comparison of the SANS pattern of the transparent GEL A (curve a) with those of an opaque gel obtained from GEL A upon aging for 960 min at room temperature (GEL B, curve b) and of an opaque gel aged for 2 weeks at room temperature, obtained by freezing a PVA/D_2O solution with $\Phi_{PVA} = 0.093$ at −22 °C for 24 h and thawing at room temperature (GEL C, curve c, redrawn from ref 15). For these gels, the inflection point at $q \approx 0.3$ nm^{-1} is indicated with arrows.

at 20 °C after 10 and 60 min of permanence of the sample at this temperature (curves b and c of Figure 2B, respectively). It is apparent that the scattered intensity decreases upon defrosting and during the storage at 20 °C and that the SANS curve obtained after 60 min at 20 °C (curve c of Figure 2B) is quite different from that of the initially homogeneous solution (curve a of Figure 2A). The solution, indeed, formed a transparent gel (GEL A).

The transparent gel obtained for low aging times at 20 °C is not thermodynamically stable. However GELA, instead of restoring the original homogeneous solution, becomes opaque within ~200 min upon standing at room temperature. The SANS pattern from the transparent GEL A (aged for 60 min at 20 °C) is compared in Figure 4 (curve a) with those of a opaque gel (GEL B) obtained from GEL A upon aging for 960 min at 25 °C (curve b) and of a opaque gel aged for 2 weeks at room temperature, obtained by freezing a PVA//D_2O solution with $\Phi_{PVA} = 0.093$ at −22 °C for 24 h and thawing at room temperature (GEL C, curve c, redrawn from ref 15). It is apparent that the scattering cross section increases with aging the gel at room temperature.

The SANS curves of PVA transparent GEL A (curve a of Figure 4) and of the opaque GEL B and GEL C (curves b and c of Figure 4) have similar shapes. In all cases, the SANS curves exhibit two distinct power law regimes, an upturn for $q < 0.08$ nm^{-1} and a knee located at $q \approx 0.3$ nm^{-1} (indicated with an arrow). Previous analyses have indicated that connectivity in GEL C is ensured by the presence of crystallites. According to these analyses, the scattering cross section of GEL C in the q range between 0.25 and 0.8 nm^{-1} (Figure 3B, curve c) is associated with the presence of PVA crystallites, whereas the inflection point at $q \approx 0.3$ nm^{-1} is related to the average distance between the crystallites of ≈20 nm ($\approx 2\pi/0.3$). Finally, the increase of scattering intensity with a power law dependence $\approx q^{-3}$, for $q < 0.08$ nm^{-1}, is associated with the mass fractal nature of the PVA network originating from the presence of polymer-rich and polymer-poor regions, where the regions occupied by the polymer-rich phase have a size on the order of micrometers and are interconnected over the macroscopic dimensions of the sample, forming a continuous phase.[15,16]

The similar shape of the scattering cross sections of the transparent GEL A and opaque GEL B (curves a and b of Figure 4, respectively) and GEL C (curve c of Figure 4) and the fact that the weight loss of these gels after one freeze/thaw cycle is below 5% with respect the weight of the initial solution[17]

possibly indicate that GELS A−C have a similar structure, i.e., that also the transparent GEL A and the opaque GEL B are characterized by the presence of heterogeneities, namely, polymer-poor and polymer-rich regions, and by the presence of crystallites or precrystalline aggregates in the polymer-rich regions. The observation that the scattering cross section of the transparent gel (GEL A) is lower than that of the opaque gels (GELS B and C) is due to the fact that the size of these heterogeneities is small in the nascent gel and increases with aging, up to becoming on the order of micrometers.[16] It is also apparent that the nonuniform structure of freeze/thaw hydrogel is imprinted during the cryogenic treatment.

It is worth noting that accurate wide-angle X-ray diffraction measurements have indicated that the size of the crystalline aggregates in the PVA hydrogels obtained by cryogenic treatments are always very small (∼3−4 nm) independent of the number of freeze/thaw cycles and of the aging time at room temperature.[17,18] Moreover, even if the degree of crystallinity tends to increase with increasing the number of freeze/thaw cycles and the aging time, it remains always below 2%. Therefore, the fact that GEL A becomes opaque upon aging at room temperature may not be ascribed to an increase of crystallinity and/or an increase of the crystallite size, but should be associated with the growth of the size of other kind of heterogeneities.

The fast cryogenic treatment, indeed, causes the formation of a transparent gel, having the same composition as the initial homogeneous solution. On the basis of the phase diagram by Komatsu et al.[1] (Figure 1), the solution containing 10% w/w PVA ($\Phi = 0.086$) is in the one-phase region and should not give rise to a gel at room temperature. However, the transparent gel obtained from this solution by cryotropic treatment at −13 °C (GEL A), does not transform back into the initial homogeneous solution, because a strong network scaffolding is already formed, due to the presence of PVA crystallites. Furthermore, GEL A is too stable to evolve toward complete elimination of the solvent.[24] GEL A, instead, reacts by increasing the size of regions that are alternatively dense and diluted (microsyneresis), i.e. the regions that are originated, upon defrosting, from the regions occupied at subzero temperature by ice and the unfrozen liquid microphase, respectively. The increase of the size of these regions is probably driven by their tendency to minimize their surface of contact. This tendency, in turn, induces a neat coarsening of the heterogeneities, with the result that GEL A becomes opaque, suggesting that spinodal decomposition occurs.[25] This phenomenon, indeed, has been observed also for other gels.[25] It generally occurs when a swollen gel is suddenly brought into another state that may be located either in the two-phase or in the one-phase region of its phase diagram.[25b] Independent of the region of the phase diagram in which the new state is located, it has been shown that the system becomes opaque without any appreciable volume change, suggesting occurrence of spinodal decomposition in both cases. However, in contrast to the usual fluids, the domain growth is slow because the elastic force of the gel suppresses the surface tension force, which is the driving force of domain growth.[25a]

The structural transformations occurring in the opaque GEL B (with $\Phi_{PVA} = 0.086$) during a successive cryotropic treatment at −13 °C were followed by TR-SANS. In Figure 5 the SANS curves from GEL B measured at 20 °C, at the beginning of freezing ($t_{freezeI} = 0$) (curve a) are compared with the SANS curves recorded after 9 (curve b) and 45 min (curve c) of permanence of this gel at −13 °C. It is apparent that the scattering cross section of GEL B increases during its permanence at −13 °C, reaching constant values after ≈45 min. It is worth noting that the SANS curve of the frozen GEL B (curve c of Figure 5, and curve d of Figure 3B) is similar to that one of the frozen solution (curve b of Figure 3B), indicating that these two systems have a similar structure. The fact that these two SANS patterns originate from different states of the same sample, i.e., the frozen solution (first freezing, curve d of Figure 2A) and the frozen GEL B (second freezing, curve c of Figure 5), confirms that the structural organization of the network scaffolding that characterizes PVA hydrogels obtained by cryotropic treatments on the length scale sampled by our SANS measurements is already obtained during the first freezing step starting from the homogeneous solution.

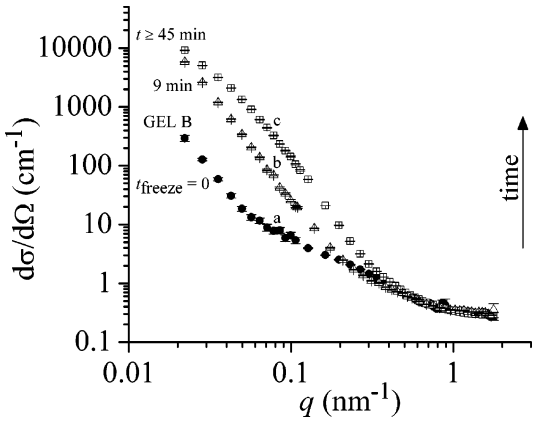

Figure 5. Change of the scattering cross section as a function of q of an opaque GEL B at 20 °C before the quenching at −13 °C ($t_{freeze} = 0$) (a) and during the permanence of GEL B at −13 °C, after 9 min (b) and 45 min (c). The elapsed time (min) after the quenching at −13 °C is indicated.

Kinetic Analysis of SANS Data. The structural changes that occur in the hydrogels obtained by application of a single freeze/thaw cycle to PVA/water solutions, during the storage of the gels at room temperature, have not been analyzed in this context. These phenomena, indeed, occur on a length scale larger than that sampled by our SANS experiments and correspond to the coarsening of regions of size higher than 300 nm, i.e., the polymer-rich and polymer-poor regions, imprinted during the cryogenic treatment. Our data, instead, allow detailed information on the structural changes occurring at nanoscale to be obtained, in the early stages of cryotropic gelation of PVA solutions.

In order to investigate the gelation kinetics in an early stage of the cryotropic gelation of PVA/water solutions, the SANS data collected from the $\Phi_{PVA} = 0.086$ solution of Figure 2A are plotted in Figure 6 as a function of time. More precisely, Figure 6 shows the change of the scattering cross section as a function of time, collected during the permanence of the homogeneous solution with $\Phi_{PVA} = 0.086$ at −13 °C, for different values of q.

It is apparent that for q values less than ∼0.1 nm^{-1} the scattering cross section appears to increase only slightly during the first 12 min at low temperature, exhibiting a sharp increase at about 12 min and becoming almost constant in the successive 300−400 min. For q values comprised between 0.1 and 0.4 nm^{-1} the scattering cross section exhibits a smooth increase in the first 20 min and does not reach any constant plateau value even after 300−400 min of permanence of the solution at −13 °C. Finally, the scattering cross section for q values higher than 0.4 nm^{-1} seems to increase rather smoothly with time. These data reflect the fact that the structural changes that occur in the solution at −13 °C in the low q range ($q < 0.1$ nm^{-1}),

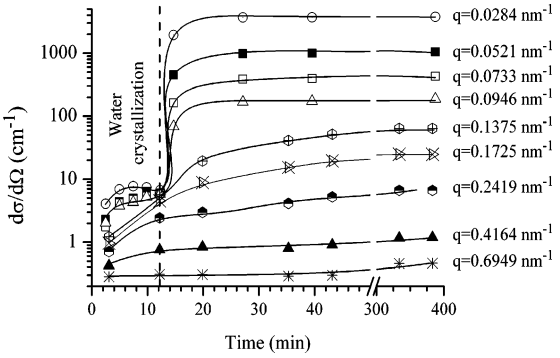

Figure 6. Change of the logarithmic scattering cross section as a function of time at the indicated values of q from the $\Phi_{PVA} = 0.086$ solution during the permanence of the solution at −13 °C. Measurements started immediately after quenching the solution at this temperature.

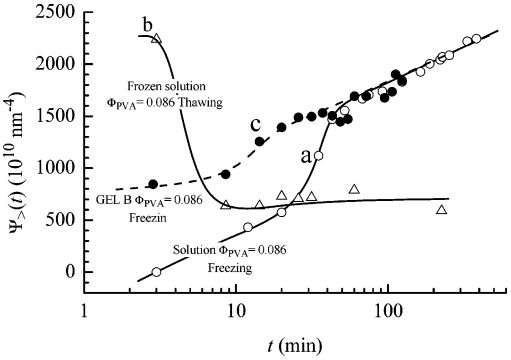

Figure 7. Reduced scattering invariant $\psi_>(t)$ as a function of time calculated from the TR-SANS measurements for $q \geq 0.108$ nm^{-1} from the solution with $\Phi_{PVA} = 0.086$ during freezing at −13 °C (○, curves a), successive thawing of the frozen solution at 20 °C (△, curve b), and subsequent freezing of GEL B at −13 °C (●, curve c).

and therefore for domains of average size larger than 100 nm ($\approx 2\pi/0.1$), are fast and are mainly associated with the crystallization of the water, which takes place in the early 10 min. At q values higher than 0.1 nm^{-1}, instead, and therefore for domains of average dimensions smaller than 100 nm, the structural transformations are much slower and are related to changes that occur in the unfrozen liquid microphase. It is worth noting that our data do not allow us to rule out the occurrence, at least in the early 10−12 min of permanence of the solution at −13 °C after quenching, of a liquid−liquid phase separation as expected from the phase diagram of Komatsu et al.[1] (Figure 1), either because the spinodal decomposition is buried by the crystallization of water and/or because, in the early stages of spinodal decomposition, concentration fluctuation corresponds to wave lengths larger than $2\pi/q_{min}$ ($\approx$300 nm).[4]

A better insight into the structural changes that occur in PVA/water solutions during the permanence of the solution at −13 °C and successive thawing at 20 °C for q higher than $\approx$0.1 nm^{-1} may be achieved with the use of the scattering invariant in the working hypothesis that, in the early stages of gelation, the scattering pattern contains additive contributions from the aggregated and nonaggregated phases and that the interactions between these two phases may be neglected. Namely, we have evaluated a reduced scattering invariant defined as the excess of scattering invariant at time t with respect to the scattering invariant of the initial solution (normalized to the volume fraction of PVA in each solution) according to the following function:

$$\psi(t) = \frac{\int_{q_{min}}^{q_{max}} q^2 \left\{ \left[\frac{\partial \sigma}{\partial \Omega}(q) \right]_t - \left[\frac{\partial \sigma}{\partial \Omega}(q) \right]_{t=0} \right\} dq}{\Phi_{PVA}} \qquad (1)$$

It is assumed that the "reduced scattering invariant" defined by eq 1 represents a measure of the "extent of aggregation phenomena" that occurs in the system, along the gelation path.

Only the SANS data collected for $q \geq 0.108$ nm^{-1} were analyzed, by setting the integration limits q_{min} and q_{max} in eq 1 equal $q_{min} = 0.108$ nm^{-1} and $q_{max} = 0.881$ nm^{-1} to obtain $\psi_>(t)$. In fact, as suggested by the SANS data plotted in Figure 6, the structural changes that occur for $q < 0.108$ nm^{-1} at correlation distances R higher than $\approx$40 nm and those occurring between 7 and 58 nm (i.e., in the unfrozen liquid microphase, for the SANS data collected for $0.108 \leq q \leq 0.881$ nm^{-1}) are different and involve different characteristic times.

The reduced scattering invariant $\psi_>(t)$ (eq 1) evaluated from the TR-SANS measurements collected during the permanence of the D_2O/PVA solutions at −13 °C (first freezing) is compared in Figure 7 with those evaluated for the successive thawing of the frozen solution at 20 °C and the subsequent freezing of GEL B at −13 °C (second freezing).

As shown in ref 21, the smoothed S-shape of the reduced scattering invariant $\psi_>(t)$ obtained from TR-SANS measurements at $q \geq 0.108$ nm^{-1} during the permanence of the solutions with $\Phi_{PVA} = 0.086$ at −13 °C (curve a of Figure 7) corresponds to the crystallization of PVA in the unfrozen liquid microphase. It is apparent that this curve increases smoothly in the first 30 min, presents a clear upturn around 30−40 min, and increases smoothly again in the successive 120−330 min of freezing, without reaching any plateau value, even for prolonged times of permanence of the systems at −13 °C. This suggests that after completion of the crystallization of the solvent (that takes about 10−15 min), the PVA chains that are mostly segregated in the unfrozen liquid microphase tend to form precrystalline or crystalline aggregates, probably because the concentration of the liquid microphase reaches the eutectic composition. However, although the temperature of the system (−13 °C) is likely below the eutectic temperature, the full crystallization of PVA may not be achieved, and it is slowed down due to the fact that the unfrozen liquid microphase jellifies, preventing the attainment of the thermodynamic equilibrium. The formation of the gel microphase may be determined by aggregation of PVA chains in a confined environment, driven by hydrogen bonding, consequent formation of crystallites, and vitrification of the swollen amorphous phase at a temperature that is likely below the glass transition.[5]

The reduced scattering invariant $\psi_>(t)$ obtained from SANS measurements taken at $q \geq 0.108$ nm^{-1} during the melting of ice in the frozen solution with $\Phi_{PVA} = 0.086$ at 20 °C and the successive permanence of this system at this temperature is reported in Figure 7 (curve b). From these data it is apparent that, during thawing, the reduced scattering invariant $\psi_>(t)$ decreases rather steeply, within approximately 10 min, reflecting the melting of ice. Afterward, the reduced scattering invariant becomes constant and higher than that of the initial solution, reflecting the fact that the system has formed a gel. Furthermore, the fact that the function $\psi_>(t)$ remains constant in this gel, indicates that at 20 °C no further crystallization of PVA takes place. This is probably due to the fact that the swelling action of the solvent on the PVA chains belonging to the amorphous phase prevents further crystallization of PVA.

The reduced scattering invariant $\psi_>(t)$ relative to GEL B is also reported in Figure 7 (curve c). It is apparent that for GEL B, $\psi_>(t)$ increases smoothly in the first 10 min, presents an

upturn around 10−15 min, and increases smoothly again in the successive 90−100 min of permanence at −13 °C. Furthermore, the values of $\psi_>(t)$ for GEL B are higher than those for the solution in the first 30 min at −13 °C and become nearly coincident with those of the solution for $t > 30$ min. This behavior reflects the fact that at the beginning of the cryotropic treatment at −13 °C, GEL B is characterized by a structure more heterogeneous that that of the corresponding initial solution and that the structure of these two systems in the frozen state becomes practically equivalent. This is also indicated by the fact that whereas the SANS curve of GEL B (curve b of Figure 4) is different from that of the initial solution (curve a of Figure 2A) the SANS curves of the two frozen systems are similar (curves b and d of Figure 3B). Most likely, PVA crystallization in the unfrozen microphase of eutectic composition is the leading phenomenon that occurs also in the case of GEL B during its permanence at −13 °C. The major difference in the two systems consists of the fact that in the case of the solutions, PVA crystallization takes place as a consequence of solvent crystallization and the concomitant formation of the unfrozen liquid microphase of eutectic composition, which in turns transforms into a microgel fraction after the first 30−40 min at −13 °C. Thereby, PVA crystallization is slowed down after the first 30−40 min of permanence of the solution at subzero temperatures.[16] In the case of GEL B, instead, during the freezing at −13 °C, the unfrozen microphase that forms in the polymer-dense regions concomitantly with the water crystallization already constitutes a gel because of its interconnected structure due to the presence of PVA crystallites that had already formed during the preceding cryotropic treatment of the initial solution at −13 °C.

The kinetics of microstructural transformations in the unfrozen liquid microphase from the PVA solutions and GEL B with $\Phi_{PVA} = 0.086$ was analyzed using the Avrami equation:

$$1 - \psi_>(t)/\psi_\infty = \exp(-kt^n) \qquad (2)$$

In agreement with the analysis performed in ref 21, the parameter used for this analysis is the ratio $\psi_>(t)/\psi_\infty$, where ψ_∞ is the value of the reduced scattering invariant for $q \geq 0.108$ nm^{-1} reached by our systems during the permanence at −13 °C at infinite time, and the ratio $\psi_>(t)/\psi_\infty$ represents the extent of PVA crystallization in the unfrozen liquid microphase.

A common value of $\psi_\infty = 4.28 \times 10^{-7}$ nm^{-4} may be obtained for the solutions and GEL B, by linear extrapolation of the reciprocal of the logarithmic scattering invariant with respect to reciprocal logarithmic time (Figure 8A).

The Avrami exponent obtained from the linear fit of Figure 8B for the solution corresponds to $n = 1$ in the first 40 min and $n = 0.25$ during the successive minutes, whereas in the case of GEL B, all data can be interpreted in terms of a unique value of the exponent $n = 0.25$. It is worth noting that the extrapolated value of ψ_∞ is an upper limit, and a change of ψ_∞ value of 20−30% does not affect very much the values of n (maximum variations being of 10−15%). This means that the determination of ψ_∞ is relatively insensitive to the kinetics.

For the frozen solution, an exponent of $n = 1$ is consistent with a one-dimensional (fibrillar) growth mechanism controlled by heterogeneous (athermal) nucleation.[26] Athermal nucleation is triggered by the active surface of ice at the interface between the ice matrix and the unfrozen liquid microphase. The low Avrami exponent of 0.25 is rather uncommon. In agreement with the arguments given in ref 21 (see also ref 27), a possible reason for a value of n lower than 1 in the later stages of crystallization kinetics of PVA in the frozen solution may be

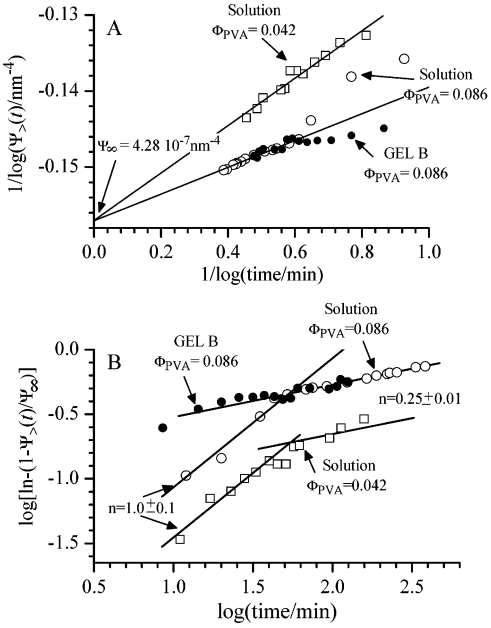

Figure 8. (A) Extrapolation of reciprocal of logarithmic scattering invariant, $[\log(\psi_>(t))]^{-1}$, with respect to reciprocal logarithmic time, $[\log(t)]^{-1}$, of the $\Phi_{PVA} = 0.086$ and 0.042 solutions and GEL B, at $[\log(t)]^{-1} = 0$, to find the scattering invariant at infinite time, ψ_∞. (B) Avrami plot of the reduced scattering invariant normalized to the values of ψ_∞ of the $\Phi_{PVA} = 0.086$ and 0.042 solutions and GEL B.

restriction of crystal growth due to the fact that previously formed PVA crystals reduce the mobility of PVA chains dissolved in the unfrozen liquid microphase. This reduced mobility, in turn, results in the jellification of the unfrozen microphase. In the case of GEL B, a low Avrami exponent occurs since the early instants that the system is kept at −13 °C due to the fact that PVA crystallization takes place in a confined environment containing crystals that had already formed during the preceding cryotropic treatment of the initial solution at −13 °C. Therefore, PVA crystallization in the frozen GEL B appears a sort of continuation of the process that was somehow interrupted by the swelling action of water, during its permanence at 20 °C. This fact explains the reason why a practical way to increase the mechanical strength of freeze/thaw PVA hydrogels consists of repeating the number of these cycles at least three to five times, through a prolonged storage of the system at subzero temperatures.[2,5,6,17−19] This procedure, indeed, induce an increase of crystallinity in the dense regions created during the first cryotropic treatment of the initial solutions, with a consequent increase of the mechanical strength.

Conclusions

The cryotropic gelation of PVA hydrogels was followed by the TR-SANS technique. The analysis of the data shows that very simple processes subtend the formation of PVA hydrogels by the freeze/thaw technique. It is clearly shown that, upon freezing an initially homogeneous PVA solution at low temperatures, the fastest process that could be detected in our approach is the crystallization of the solvent. Water crystallization induced a progressive increase of the concentration in PVA in the surrounding solution, reaching the eutectic composition. The eutectic solution that forms at low temperature (below −10 °C) constitutes the so-called unfrozen liquid microphase, where the crystallization of PVA takes place. However, although the temperature of the system (−13 °C) is likely below the eutectic temperature, the crystallization of PVA may not be complete,

because the unfrozen liquid microphase jellifies, preventing the attainment of the thermodynamic equilibrium. The formation of the microgel fraction is due to formation of crystallites acting as physical cross-links, and/or to the vitrification of the swollen amorphous phase surrounding the crystallites, at temperature below the glass transition.

Upon thawing, ice crystals melt, yielding a transparent gel only for solutions having a concentration higher than a critical value. Indeed, two conditions must be fulfilled in order to have a gel: the droplets of unfrozen liquid microphase should form a network cluster inside the ice matrix (i.e., they should be at a concentration higher than a percolation threshold), and the size of the precrystallite or crystallite aggregates that form inside the microphase should be higher than a critical value.

The transparent gels become opaque upon aging at room temperature, due to a coarsening of the heterogeneous structure imprinted by the cryotropic treatment, consisting of an alternation of diluted and dense regions. Dense and diluted regions originate upon defrosting from the regions occupied by ice and the unfrozen liquid microphase, respectively. This transformation is driven by the tendency of the dense and dilute regions to minimize their surface of contact.

During the permanence of these gels at room temperature (hours), the presence of a high content of water (higher than 85% by mass) prevents further crystallization of PVA, due to its swelling action. At this temperature, the less stable crystallites that had formed at subzero temperature, are probably dissolved by water, resulting in a decrease of the degree of crystallinity. Crystallization of PVA, in turn, is resumed by freezing the gels at subzero temperatures, after water crystallization and consequent formation of an unfrozen microgel fraction.

In the Introduction, the strong structural analogies between our gels with the PVA gels obtained in 60/40 v/v DMSO/water mixtures[12] were already discussed. However, the present investigation points out that whereas the phase-separated structure of the gels of ref 12 is due to a liquid−liquid phase separation that takes place before gelation, in cryotropic PVA hydrogels the heterogeneous structure is imprinted by incomplete crystallization of solvent and consequent formation of an unfrozen liquid microphase more concentrated in PVA. Therefore, in cryotropic PVA hydrogels, the regions that are alternatively dense and diluted originated, upon defrosting, from the regions occupied at subzero temperature by ice and the unfrozen liquid microphase, respectively.

Our SANS approach has allowed us to reach an unprecedented level of comprehension of the complex phenomena subtending the cryotropic gelation of PVA/water solutions. Such information may turn out to be very useful to improve the processing conditions for obtainment of polymer-based hydrogels with an open porous structure typically used in biotechnology and for biomedical applications.

Acknowledgment. This research project has been supported by the European Commission under the Sixth Framework Programme through the Key Action: Strengthening the European Research Area, Research Infrastructures (Contract No.: RII3-CT-2003-505925).

References and Notes

(1) Komatsu, M.; Inoue, T.; Miyasaka, K. *J. Polym. Sci. B: Polym. Phys.* **1986**, *24*, 303.

(2) Kawanishi, K.; Komatsu, M.; Inoue, T. *Polymer* **1987**, *28*, 980.

(3) Bunn, C. W. *Nature* **1948**, *161*, 929.

(4) Cahn, J. W. *J. Chem. Phys.* **1965**, *42*, 93.

(5) Hassan, C. M.; Peppas, N. A. *Adv. Polym. Sci.* **2000**, *153*, 37.

(6) Lozinsky, V. I. *Russ. Chem. Rev.* **1998**, *67*, 573; Lozinsky, V. I.; Galaev, I. Y.; Plieva, F. M.; Savina, I. N.; Jungvid, H.; Mattiasson, B. *Trends Biotechnol.* **2003**, *21*, 445.

(7) Peppas, N. M. *Makromol. Chem.* **1975**, *176*, 3433; Stauffer, S.; Peppas, N. A. *Polymer* **1992**, *33*, 3932.

(8) Lozinsky, V. I.; Damshkaln, L. G. *J. Appl. Polym. Sci.* **2000**, *77*, 2017.

(9) Willcox, P. J., Jr.; Howie, D. W., Jr.; Schmidt-Rohr, K.; Hoagland, D. A.; Gido, S. P.; Pudjijanto, S.; Kleiner, L. W.; Venkatraman, S. *J. Polym. Sci., Part B: Polym. Phys.* **1999**, *37*, 3438.

(10) Kanaya, T.; Ohkura, M.; Kaji, H.; Furusaka, M.; Misawa, M. *Macromolecules* **1994**, *27*, 5609−5615.

(11) Kanaya, T.; Takeshita, H.; Nishikoji, Y.; Ohkura, M.; Nishida, K.; Kaji, K. *Supramol. Sci.* **1998**, *5*, 215−221.

(12) Kanaya, T.; Ohkura, M.; Takeshita, H.; Kaji, H.; Furusaka, M.; Yamaoka, H.; Wignall, G. D. *Macromolecules* **1995**, *28*, 3168−3174.

(13) Takeshita, H.; Kanaya, T.; Nishida, K.; Kaji, K. *Physica B* **2002**, *311*, 78−83.

(14) Takeshita, H.; Kanaya, T.; Nishida, K.; Kaji, K. *Macromolecules* **1999**, *32*, 7815−7819.

(15) Ricciardi, R.; Mangiapia, G.; Lo Celso, F.; Paduano, L.; Triolo, R.; Auriemma, F.; De Rosa, C.; Lauprêtre, F. *Chem. Mater.* **2005**, *17*, 1183.

(16) Mangiapia, G.; Ricciardi, R.; Auriemma, F.; De Rosa, C.; Lo Celso, F.; Triolo, R.; Heenan, R. K.; Radulescu, A.; Tedeschi, A. M.; D'Errico, G.; Paduano, L. *J. Phys. Chem. B* **2007**, *111*, 2166.

(17) Ricciardi, R.; Auriemma, F.; De Rosa, C.; Lauprêtre, F. *Macromolecules* **2004**, *37*, 1921.

(18) Ricciardi, R.; Auriemma, F.; Gaillet, C.; De Rosa, C.; Lauprêtre, F. *Macromolecules* **2004**, *37*, 9510.

(19) Ricciardi, R.; D'Errico, G.; Auriemma, F.; Ducouret, G.; Tedesch, i A. M.; De Rosa, C.; Laupretre, F.; Lafuma, F. *Macromolecules* **2005**, *38*, 6629.

(20) Tedeschi, A.; Auriemma, F.; Ricciardi, R.; Mangiapia, G.; Trifuoggi, M.; Franco, L.; De Rosa, C.; Heenan, R. K.; Paduano, L.; D'Errico, G. *J. Phys. Chem. B* **2006**, *110*, 23031.

(21) Auriemma, F.; De Rosa, C.; Triolo, R. *Macromolecules* **2006**, *39*, 9429.

(22) Matsuo, M.; Kawase, M.; Sugiura, Y.; Takematsu, S.; Hara, C *Macromolecules* **1993**, *26*, 4461.

(23) Emmerling, A.; Petricevic, R.; Beck, A.; Wang, P.; Scheller, H.; Fricke, J. *J. Non-Cryst. Sol.* **1995**, *185*, 240.

(24) de Gennes, P.-G. *Scaling Concepts in Polymer Physics;* Cornell University Press: Ithaca, NY, 1979.

(25) (a) Hirotsu, S.; Kaneki, A. In *Dynamics of Ordering Process in Condensed Matter*; Komura, S., Furukawa, H., Eds.; Plenum: Kyoto, 1988; pp 481−486. (b) Takeshita, H.; Kanaya, T.; Nishida, K.; Kaji, K. *Macromolecules* **2001**, *34*, 7894.

(26) Wunderlich, B. *Macromolecular Physics, Crystal Melting;* Academic Press: New York, 1980; Vol. 3.

(27) Grebowicz, J.; Cheng, S. Z. D.; Wunderlich, B. *J. Polym. Sci., Part B: Polym. Phys.* **1986**, *24*, 675; Cheng, S. Z. D. *Macromolecules* **1988**, *21*, 2475.